

NUMERICAL ASPECTS OF THERMO-MECHANICAL COUPLED PROBLEMS

Miguel Vaz Júnior - dem2mvj@joinville.udesc.br

Departamento de Engenharia Mecânica, Centro de Ciências Tecnológicas,
Universidade do Estado de Santa Catarina (UDESC), 89223-100 - Joinville/SC, Brasil

***Abstract.** Thermo-mechanical coupling is the most common class of coupled problems, in which the mechanical response of the structure depends on its thermal behaviour and vice-versa. The ability to solve these problems successfully is crucially linked to the mechanical and thermal inter-dependence modelling strategy employed. Particularly for large-scale problems, a staggered solution approach is generally adopted, in which separate analyses are undertaken for each phenomenon with data exchange performed at a pre-defined time or increment intervals. The present work discusses the thermodynamics of a thermoplastic model in association with a large strain/large displacement elastoplastic model aiming application at metal forming problems.*

***Keywords:** Thermo-mechanical coupling, Finite Elements, Computational Plasticity*

1. INTRODUCTION

Thermo-mechanical coupling is the most common class of coupled problems, in which the mechanical response of the structure depends on its thermal behaviour and *vice-versa*. The ability to solve these problems successfully is crucially linked to the mechanical and thermal inter-dependence modelling strategy employed. Particularly for large problems, a staggered solution approach is generally adopted, in which separate analyses are undertaken for each phenomenon with data exchange performed at a pre-defined time or increment intervals.

The independent solution of heat transfer problems is reasonably well established and does not present any substantial difficulties even if non-linearities are included. Application of numerical techniques to mechanical problems has developed rapidly in the last ten years, but the critical issue of solving practical thermo-mechanical problems still seems to be open, particularly those involving large strains, large displacements, multi-fracturing materials, complex friction/contact conditions and other complexities. Therefore, aiming application at such problems, an efficient and relatively simple thermo-mechanical algorithm using a staggered solution procedure is implemented, in which large strains and dissipation of plastic work are accounted for.

2. THERMO-MECHANICAL COUPLING

Conceptually, thermo-mechanical coupling is manifested through mutual inter-dependence of the *mechanical* and *thermal* laws. The thermal laws, represented by the *first* (energy conservation) and *second* (irreversible thermodynamics) principles of thermodynamics, govern the evolution of the temperature field, thereby affecting the material parameters and causing thermal expansion. The mechanical laws, expressed in terms of the *momentum equations*, affect the thermal problem through, primarily, the geometry change, dissipation of plastic and frictional work and thermal contact. In the present work, emphasis is given to modelling the thermal effect of the inelastic deformation.

2.1 Thermal effect of the inelastic deformation

Application of the *first* and *second principles* of thermodynamics to a body undergoing inelastic deformation leads to

$$\rho c \dot{\theta} - q_i - \rho r + \text{div}[\mathbf{q}_k] = 0 \quad (1)$$

where \mathbf{q}_k is the *Fourier law of conductivity*, $\mathbf{q}_k = -\mathbf{k}\nabla\theta$, r is a heat source other than that caused by any mechanical effect, $\dot{\theta}$ is the temperature rate, ρ , c and \mathbf{k} are the specific mass, specific heat and thermal conductivity tensor respectively and q_i represents the *inelastic coupling term*, which accounts for the thermal effect of the inelastic deformation. It is interesting to note q_i can assume different forms according to the thermoplastic model adopted (Argyris & Doltsinis, 1981; Perzyna, 1993).

3. LARGE DEFORMATION ELASTOPLASTICITY

The mechanical solution of large strain/large deformation elastoplastic problems requires complex mathematical and numerical tools to account for geometrical nonlinearities. The classical approach to small strain problems uses the so-called additive decomposition of the strain tensor, $\boldsymbol{\varepsilon} = \boldsymbol{\varepsilon}^e + \boldsymbol{\varepsilon}^p$, into elastic, $\boldsymbol{\varepsilon}^e$, and plastic, $\boldsymbol{\varepsilon}^p$, components. On the other hand, its

use in large deformation problems leads to other difficult problems, such as definition of robust objective stress rate tensors, which still is a matter of intense discussion. In recent years, an approach based on multiplicative decomposition of the *deformation gradient* tensor (Lee, 1969), \mathbf{F} , has been proposed as

$$\mathbf{F} = \mathbf{F}^e \mathbf{F}^p \quad (2)$$

in which \mathbf{F}^e and \mathbf{F}^p represent the elastic and plastic components of the deformation gradient. Furthermore, the *velocity gradient*, $\mathbf{L} \equiv \dot{\mathbf{F}} \mathbf{F}^{-1}$, is defined from equation (2), which can also be decomposed into elastic and plastic components, $\mathbf{L} = \mathbf{L}^e + \mathbf{L}^p$, where $\mathbf{L}^e = \dot{\mathbf{F}}^e \mathbf{F}^{-e}$ and $\mathbf{L}^p = \mathbf{F}^e \dot{\mathbf{F}}^p \mathbf{F}^{-p} \mathbf{F}^{-e}$. Similarly, the *rate of deformation* (or plastic stretching) tensor, $\mathbf{D} \equiv \text{sym}[\mathbf{L}]$, is decomposed into elastic and plastic as

$$\mathbf{D} = \mathbf{D}^e + \mathbf{D}^p \quad (3)$$

in which $\mathbf{D}^e = \text{sym}[\mathbf{L}^e]$ and $\mathbf{D}^p = \text{sym}[\mathbf{L}^p]$. Therefore, the *plastic* contribution to the *rate of deformation* on the intermediate configuration is given by

$$\bar{\mathbf{D}}^p = \text{sym}[\bar{\mathbf{L}}^p] \quad (4)$$

where $\bar{\mathbf{L}}^p$ is the *plastic* contribution to the *velocity gradient*, $\bar{\mathbf{L}}^p = \dot{\mathbf{F}}^p \mathbf{F}^{-p}$. The present finite element formulation uses the *spatial* configuration to formulate the constitutive equations thereby requiring definition of the rotation of $\bar{\mathbf{D}}^p$ as

$$\tilde{\mathbf{D}}^p = \mathbf{R}^e \bar{\mathbf{D}}^p \mathbf{R}^{eT} = \mathbf{R}^e \text{sym}[\dot{\mathbf{F}}^p \mathbf{F}^{-p}] \mathbf{R}^{eT} \quad (5)$$

in which $\tilde{\mathbf{D}}^p$ is the *modified plastic stretching*, \mathbf{R}^e is the *elastic rotation*, resulting from the polar decomposition of \mathbf{F}^e , $\mathbf{F}^e = \mathbf{R}^e \mathbf{U}^e = \mathbf{V}^e \mathbf{R}^e$, where \mathbf{U}^e and \mathbf{V}^e denote the *right* and *left stretch* tensors respectively. Further considerations on the formulation summarised above can be found in De Souza Neto *et al.* (1998).

4. THERMOPLASTIC MODEL

Thermoplastic models can be derived from the thermodynamic analysis of deforming bodies in conjunction with phenomenological observations. There exists at least three general presentations, i.e., the classical *theory of irreversible processes*, the so-called *rational thermodynamics* and the *thermodynamics with internal variables*. The thermodynamic characteristics of a model, such as thermodynamic equilibrium, description of thermodynamic state and axioms, in conjunction with phenomenological considerations define individual thermoplastic formulations. The reader is referred to the following papers for further considerations on the existing thermoplastic models: Rebelo & Kobayashi (1980), Argyris & Doltsinis (1981), Simo & Miehe (1992), Perzyna (1993) and Casey (1998).

The following sections present a brief review of some basic principles and definitions and a discussion on the thermodynamics of plastic deformations under the framework of large deformation elastoplasticity using multiplicative decomposition of the *deformation gradient* tensor.

4.1 Basic principles and definitions

The derivation of an equation able to describe the temperature evolution involves the first and second principles of thermodynamics, Clausius-Duhem inequality, and definition of internal variables and thermodynamic potentials.

The *first principle of thermodynamics* expresses the conservation of energy, which applied to a continuous deformable body, can be written as

$$\rho \dot{e} = \boldsymbol{\sigma} : \mathbf{D} - \text{div}[\mathbf{q}_k] + \rho r \quad (6)$$

where \dot{e} is the internal energy rate.

The *Clausius-Duhem Inequality* is a landmark in the development of any thermoplastic model and represents a restraint to a so-called *admissible* thermodynamic process. The derivation of the *inequality* is based on the *first* and *second principles* of thermodynamics as

$$\boldsymbol{\sigma} : \mathbf{D} - \rho (\eta \dot{\theta} + \dot{\psi}) + \theta \mathbf{q}_k \cdot \text{div} \left[\frac{1}{\theta} \right] \geq 0 \quad (7)$$

where ψ is the *specific free energy*, also known as *Helmholtz specific free energy*, which is a *thermodynamic potential* associated to the internal energy and is defined by

$$\psi = e - \theta \eta \quad (8)$$

in which

$$\eta = -\frac{\partial \psi}{\partial \theta} \quad \text{and} \quad \theta = \frac{\partial e}{\partial \eta} \quad (9)$$

4.2 The temperature evolution equation

A general thermoplastic formulation, represented by the thermal evolution equation, is derived from the definition of the *total dissipation*, ϕ , which in turn, is derived from the *Clausius-Duhem Inequality* and the *first principle of thermodynamics*. Furthermore, due to the large plastic deformation, the *Cauchy* stresses, $\boldsymbol{\sigma}$, are not suitable thereby requiring use of a different approach. Therefore, the *Kirchoff* stress tensor, $\boldsymbol{\tau}$, is used in the present finite element model as

$$\boldsymbol{\tau} = \frac{\rho_0}{\rho} \boldsymbol{\sigma} \quad (10)$$

where ρ_0 is the specific mass at original configuration and ρ is the current specific mass. Therefore, the conservation of energy equation (6) can be rewritten as

$$\rho \dot{e} = \frac{\rho}{\rho_0} \boldsymbol{\tau} : \mathbf{D} - \text{div}[\mathbf{q}_k] + \rho r \quad (11)$$

The total dissipation can be defined from the *Clausius-Duhem Inequality* in conjunction with equation (10) as

$$\phi = \underbrace{\boldsymbol{\tau} : \mathbf{D} - \rho_0 (\eta \dot{\theta} + \dot{\psi})}_{\text{Intrinsic dissipation}} + \underbrace{\frac{\rho_0}{\rho} \boldsymbol{\theta} \mathbf{q}_k \cdot \text{div} \left[\frac{1}{\boldsymbol{\theta}} \right]}_{\text{Thermal dissipation}} \geq 0 \quad (12)$$

The total dissipation can be split into *intrinsic*, ϕ_{intr} , and *thermal*, ϕ_{ther} , components, as shown in equation (12). The former is due to the inelastic deformation of the system and the latter to heat transfer effects. Additionally, the rate of the *Helmholtz specific free energy*, $\dot{\psi}$, is obtained from equation (8) as

$$\dot{\psi} = \frac{\partial \psi}{\partial t} = \frac{\partial (e - \theta \eta)}{\partial t} = \dot{e} - \theta \dot{\eta} - \eta \dot{\theta} \quad (13)$$

Thus, the *intrinsic dissipation* is defined from equations (12) and (13) as

$$\phi_{intr} = \rho_0 \theta \dot{\eta} - \rho_0 \dot{e} + \boldsymbol{\tau} : \mathbf{D} \quad (14)$$

By combining the *energy equation* (11) and (14), one obtains

$$\frac{\rho_0}{\rho} \text{div}[\mathbf{q}_k] + \rho_0 \theta \dot{\eta} - \rho_0 r - \phi_{intr} = 0 \quad (15)$$

which represents the *temperature evolution equation*. However, the *specific entropy rate*, $\dot{\eta}$, and the *intrinsic dissipation*, ϕ_{intr} , still have to be determined.

Firstly, the *specific entropy rate*, $\dot{\eta}$, can be determined by using the definitions associated to the *specific free energy* (9)_a and by assuming that $\psi = \psi(\boldsymbol{\varepsilon}^e, \boldsymbol{\alpha}, \theta)$, where $\boldsymbol{\varepsilon}^e$ is the elastic strain tensor and $\boldsymbol{\alpha}$ is a set of internal variables¹. Thus

$$\rho_0 \dot{\eta} = \rho_0 \frac{\partial}{\partial t} \left(- \frac{\partial \psi}{\partial \theta} \right) = - \frac{\partial \boldsymbol{\tau}}{\partial \theta} : \dot{\boldsymbol{\varepsilon}}^e - \frac{\partial \mathbf{A}}{\partial \theta} \cdot \dot{\boldsymbol{\alpha}} + \rho_0 \frac{c}{\theta} \dot{\theta} \quad (16)$$

so that

$$\boldsymbol{\tau} = \rho_0 \frac{\partial \psi}{\partial \boldsymbol{\varepsilon}^e} \quad , \quad \mathbf{A} = \rho_0 \frac{\partial \psi}{\partial \boldsymbol{\alpha}} \quad \text{and} \quad c = -\theta \frac{\partial^2 \psi}{\partial \theta^2} \quad (17)$$

where c is the *specific heat* and \mathbf{A} is the *thermodynamical force* conjugate to the internal variables $\boldsymbol{\alpha}$.

¹ The *internal variables*, collectively denoted by $\boldsymbol{\alpha}$, are assumed to describe, macroscopically or microscopically, the internal structure of the material and can be expressed in terms of scalar, vector, tensor or n -vector. Furthermore, an evolution law, frequently represented in rate form, is associated with the problem (See Maugin, 1992; Lubliner, 1990; Perzyna, 1993, and references therein).

The first step to obtain an expression for the *intrinsic dissipation*, ϕ_{intr} , is to derive the *specific free energy*, $\psi = \psi(\boldsymbol{\varepsilon}^e, \boldsymbol{\alpha}, \theta)$, with respect to time as

$$\rho_0 \dot{\psi} = \rho_0 \frac{\partial \psi}{\partial t}(\boldsymbol{\varepsilon}^e, \boldsymbol{\alpha}, \theta) = \rho_0 \frac{\partial \psi}{\partial \boldsymbol{\varepsilon}^e} : \dot{\boldsymbol{\varepsilon}}^e + \rho_0 \frac{\partial \psi}{\partial \boldsymbol{\alpha}} : \dot{\boldsymbol{\alpha}} + \rho_0 \frac{\partial \psi}{\partial \theta} : \dot{\theta} \quad (18)$$

in which the derivative terms of the right hand side of equation (18) can be easily identified with the definitions of the Kirchoff stress tensor, $\boldsymbol{\tau}$, thermodynamical forces conjugate to internal variables, \mathbf{A} , and entropy, $\rho_0 \eta$. It is also possible to show that, for large strain elastoplasticity (De Souza Neto, 1998),

$$\frac{\partial \psi}{\partial \boldsymbol{\varepsilon}^e} : \boldsymbol{\varepsilon}^e = \frac{\partial \psi}{\partial \boldsymbol{\varepsilon}^e} : (\mathbf{D} - \tilde{\mathbf{D}}^p) \quad (19)$$

where $\tilde{\mathbf{D}}^p$ is the modified plastic stretching, which corresponds to a measure of rate of plastic deformation at large plastic strains. Therefore, the substitution of (19) into (18) yields

$$\rho_0 \dot{\psi} = \boldsymbol{\tau} : (\mathbf{D} - \tilde{\mathbf{D}}^p) + \mathbf{A} \cdot \dot{\boldsymbol{\alpha}} - \rho_0 \eta \dot{\theta} \quad (20)$$

The intrinsic dissipation can be finally obtained by combining its definition from equation (12) and equation (20) as

$$\begin{aligned} \phi_{intr} &= -\rho_0 \eta \dot{\theta} - \rho_0 \dot{\psi} + \boldsymbol{\tau} : \mathbf{D} \\ &= -\rho_0 \eta \dot{\theta} - \left[\boldsymbol{\tau} : (\mathbf{D} - \tilde{\mathbf{D}}^p) + \mathbf{A} \cdot \dot{\boldsymbol{\alpha}} - \rho_0 \eta \dot{\theta} \right] + \boldsymbol{\tau} : \mathbf{D} \\ &= \boldsymbol{\tau} : \tilde{\mathbf{D}}^p - \mathbf{A} \cdot \dot{\boldsymbol{\alpha}} \geq 0 \end{aligned} \quad (21)$$

Finally, a general *temperature evolution equation* is obtained by substituting equations (16) for the *specific entropy rate* and equation (21), for the *intrinsic dissipation* into equation (15) so that

$$\rho c \dot{\theta} - \frac{\rho}{\rho_0} \left[\boldsymbol{\tau} : \tilde{\mathbf{D}}^p - \mathbf{A} \cdot \dot{\boldsymbol{\alpha}} + \theta \left(\frac{\partial \boldsymbol{\tau}}{\partial \theta} : \dot{\boldsymbol{\varepsilon}}^e - \frac{\partial \mathbf{A}}{\partial \theta} \cdot \dot{\boldsymbol{\alpha}} \right) \right] - \rho r + \text{div}[\mathbf{q}_k] = 0 \quad (22)$$

The formulation based on *internal variables* can be applied to different materials and problems by selecting them accordingly. The complexities which arise in this formulation are due not only to a proper choice of *internal variables*, but also to the correct and consistent formulation of the dependency of these variables on the other parameters involved. Furthermore, the dependency of the stress tensor on the temperature, also known as the *thermoelasticity*, requires a proper modelling.

Aiming application at metal forming problems, a simple thermoplastic approach is adopted, which assumes that the temperature effects on stresses and rate of internal variables are negligible when compared to the dissipation of the plastic work. Therefore, equation (22) is reduced to

$$\rho c \dot{\theta} - \xi \frac{\rho}{\rho_0} \boldsymbol{\tau} : \tilde{\mathbf{D}}^p - \rho r + \text{div}[\mathbf{q}_k] = 0 \quad (23)$$

in which ξ is the *dissipation factor*, which estimates the fraction of the inelastic energy effectively transformed into heat and ranges from 0 to 1 (Taylor & Quinney, 1933). It is worth noting that this approach is valid for problems where the level of plastic deformation is much greater than the level of the elastic components of the elastic strain tensor, as in metal forming problems. Similar assumptions were adopted by Sekhon & Chenot (1993), Miles *et al.* (1995), Owen *et al.* (1995) and Vaz Jr. & Owen (1997) under the framework of small strain elastoplasticity.

5. NUMERICAL EXAMPLE

The numerical example presented in this section aims to assess the model described previously by comparing nodal temperatures computed during the upset of a cylindrical billet. The simulation of the upsetting of a cylinder using *elasto-plastic* materials, although apparently simple, requires high-level numerical tools, such as large-strain algorithms and element architecture capable of hourglass control.

One of the first numerical studies of thermo-mechanical analysis using the upsetting problem was reported by Rebelo & Kobayashi (1980). Since then, Rebelo and Kobayashi's test case has become one of the most common benchmark when assessing thermo-mechanical coupled problems. A very diligent analysis was presented by Tugcu (1996) who evaluate effects of the thermal softening and strain rate using an elasto-viscoplastic material model and hypoelastic formulation. Further studies aiming at application to hot and cold forging, using the upsetting example, were presented by César de Sá *et al.* (1996) and Pantuso & Bathe (1997). The former adopted a rigid-viscoplastic material model in conjunction with a mixed finite element formulation, whereas the latter emphasised aspects of mechanical and thermal contact. This brief review shows the relevance of the problem adopted to assess the present thermo-mechanical model.

5.1 Problem description

The geometry of the problem and the finite element mesh are depicted in Figure 1. Due to symmetry, only one quarter of the billet and half of the upper die are modelled. Table 1 summarises the data for carbon steel AISI 1015 and other parameters used in the simulation. In order to reduce the effects of other phenomena, a high frictional coefficient is assumed, which virtually eliminates any relative movement between the dies and the workpiece. The mechanical solution is obtained using finite elements in conjunction with an implicit time integration scheme, associated with an elasto-plastic material model based on the multiplicative decomposition of the deformation gradient tensor. The temperature distribution is determined using an adiabatic heating approach.

The upsetting is achieved by applying 5 mm (1/3 compression of the original cylinder height) downward rigid surface movement to the upper die. In order to simulate a mechanical press, the compression speed (relative velocity between dies, v) decreases towards the end of the operation as

$$v(t) = 12 \sqrt{H(t) - 20} \quad (24)$$

where $H(t)$ is the total billet height (Rebelo & Kobayashi, 1980).

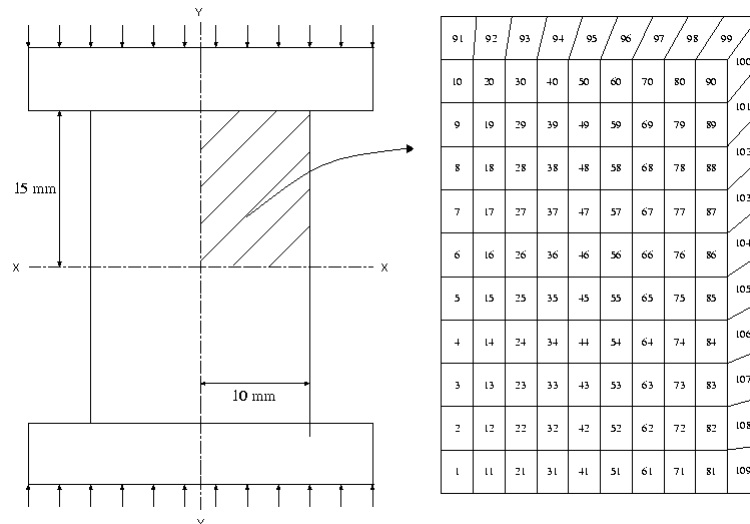


Figure 1. Geometry of the problem and Finite Element Mesh.

Table 1. Material properties and other simulation parameters.

Description	Symbol	Value
Specific mass	ρ	7800 kg/m^3
Specific heat	c	483.3 J/kg K
Thermal conductivity	k	36.0 J/m K
Friction coefficient	μ	0.6
Young's Modulus	E	200 GPa
Poisson's ratio	ν	0.3
Yield stress	σ_Y	$722(\bar{\epsilon}_p + 0.02512)^{0.262} \text{ MPa}$
Dissipation factor	ξ	0.75
Coupling interval		
Explicit	Δt	0.01 s
Implicit	-	every solution increment
Present work	-	every solution increment

5.2 Simulation results

In metal forming processes, dissipation of the inelastic work generates thermal energy, which in turn, causes an increase of the workpiece temperature. In addition, the adiabatic approach assumes that the heat generated remain localised, whose approximation can be safely adopted in problems of low thermal diffusibility or processes of short duration.

Validation of the model is performed by comparing nodal implicit and explicit solutions provided by a general purpose finite element code (Elfen,1996) for a point at the centre of the billet, as presented in Table 2. It has been found that, in general, the divergences from Elfen's solutions increase with increasing compression. The differences with the *implicit* module increases from 0.12 %, at the first load increment, to 0.64 %, at the end of the compression process. As expected, the discrepancies presented by the *explicit* module are greater, increasing from 0.12 % to 2.41 % towards the end of the process. The divergence between the *implicit* and *explicit* solutions is caused by the integration strategy of the mechanical problem. The former requires a converged solution at every load increment whereas the latter is

approximated by an explicit time integration scheme thereby avoiding an iterative procedure, but requiring much smaller time steps.

Table 2. Temperature distribution at the cylinder centre at $t = 0.5$ s.

Compression [mm]	Time [s]	Temperature [K]		
		Explicit (Elfen, 1996)	Implicit (Elfen, 1996)	Present work
0.00000	0.000	292.00	292.00	292.00
0.46310	0.025	295.59	295.28	295.23
0.90370	0.050	299.79	299.15	299.08
1.71735	0.100	309.19	307.92	307.78
2.44105	0.150	319.22	317.82	317.56
3.07475	0.200	329.26	328.49	328.00
3.61840	0.250	338.74	339.40	338.57
4.07210	0.300	347.19	349.86	348.64
4.43580	0.350	354.39	359.19	357.56
4.70945	0.400	360.13	366.79	364.79
4.89315	0.450	364.14	372.15	369.89
5.00000	0.500	366.53	375.37	372.94

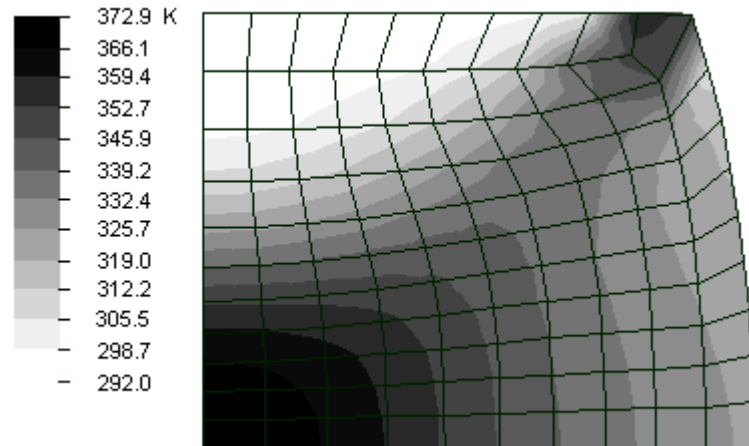


Figure 2. Temperature distribution at $t = 0.5$ s.

Figure 2 shows the temperature distribution in the workpiece at $t = 0.5$ s. The highest temperatures are found near the centre of the workpiece, which are caused by the high plastic deformation at this region. It worth noting that the high friction coefficient assumed in the simulations causes a very small relative displacement between the dies and the workpiece faces, which virtually eliminates the heat generation due to the dissipation of frictional work.

6. FINAL REMARKS

This paper presents a general thermoplastic model aiming application at metal forming processes. The general model is derived from the first and second principles of thermodynamics in conjunction with the Clausius-Duhem inequality and based on internal

variables. The mathematical formulation accounts for large strains/large deformation based on the multiplicative decomposition of the gradient velocity tensor. The validation of the model is performed by comparing the temperature distribution with solutions provided by a general purpose finite element code. Due to the implicit nature of the present solution, the divergences with Elfen's implicit module were significantly smaller than its explicit counterpart.

REFERENCES

- Argyris, J.H. & Doltsinis, J.S., 1981, On the Natural Formulation and Analysis of Large Deformation Coupled Thermomechanical Problems, *Comp. Meth. Appl. Mech. Eng.*, v. 25, pp. 195-253.
- Casey, J., 1998, On Elastic-Thermo-Plastic Materials at Finite Deformations, *Int. J. Plasticity*, v.14, pp.173-191.
- César de Sá, J., Sousa, L.C. and Madureira, M.L., 1996, Simulation Model for Hot and Cold Forging by mixed Methods including Adaptive Mesh Refinement, *Engng. Comp.* v. 13, pp. 339-360.
- De Souza Neto, E.A., Perić, D. and Owen, D.R.J., 1998, Continuum Modelling and Numerical Simulation of Material Damage at Finite Strains, *Arch. Comput. Meth. Engng.*, v.5, pp. 311-384.
- Lee, E.H., Elastic Plastic deformation at Finite Atrains, *J. Appl. Mech.*, v. 36, pp. 1-6.
- Lubliner, 1990, *J. Plasticity Theory*, Macmillan, New York.
- Maugin, G.A., 1992, *The Thermo-Mechanics of Plasticity and Fracture*, Cambridge University Press, Cambridge.
- Miles, M.P., Fourment, L. and Chenot, J.L., 1995, Finite Element Calculation of Thermal Coupling between Workpiece and Tools in Forging, *Engng. Comp.*, v. 12, pp. 687-705.
- Owen, D.J.R., Perić, D., Crook, A.J.L., De Souza Neto, E.A., Yu, J. and Dutko, M., 1995, Advanced Computational Strategies for 3-D Large Scale Metal Forming Simulations, in *Numerical Methods in Industrial Forming Processes*, New York.
- Pantuso, D. & Bathe, K.J., 1997, Finite Element Analysis of Thermo-Elasto-Plastic Solids in Contact, eds. D.R.J. Owen, E. Oñate and E. Hinton, CIMNE, Barcelona, pp. 72-87.
- Perzina, P., 1993, Constitutive Equations for Thermoinelasticity and Instability Phenomena in Thermodynamic Flow Processes, in *Progress in Computational Analysis of Inelastic Structures*, ed. E. Stein, Springer-Verlag, Wien, pp. 1-78.
- Rebelo, N. & Kobayashi, S., A., 1980, Coupled Analysis of Viscoplastic Deformation and Heat Transfer - I and II, *Int. J. Mech. Sci.*, v. 22, pp. 699-718.
- Rockfield Software Ltd., 1996, *Elfen - User manual*, Swansea.
- Sekhon, G.S. & Chenot, 1993, J.L., Numerical Simulation of Continuous Chip Formation During Non-Steady Orthogonal Cutting, *Engng. Comp.*, v.10, pp.31-48.
- Simo, J.C. & Miehe, 1992, C. Associative Coupled Thermoelasticity at Finite Strains: Formulation, Numerical Analysis and Implementation, *Comp. Meth. Appl. Mech. Eng.*, v. 98, pp.41-104.
- Taylor, L.M. & Quinney, H., 1933-34, The latent energy remaining in a metal after cold working, *Proc. R. Soc. Lond.*, v. A 143, pp. 307-326.
- Tugcu, P., 1996, Thetrmomechanical Analysis of Upsetting of a Cylindrical Billet, *Comp. & Struc.*, v. 58, pp.1-12.
- Vaz Jr., M. & Owen, D.J.R., 1997, Thermo-mechanical Coupling and Large-scale Elasto-plastic Problems, in *Application of Numerical Methods in Engineering*, eds. S. Basri, A.A.A. Samad and A.M. Hamouda, UPM Press, Serdang, pp. 377-388.